



Cite this: *Dalton Trans.*, 2014, **43**, 15313

Received 25th April 2014,
Accepted 19th August 2014

DOI: 10.1039/c4dt01210k

www.rsc.org/dalton

Dihaloborenum cations stabilized by a four-membered N-heterocyclic carbene: electron deficiency compensation by asymmetric structural changes†

Madelyn Qin Yi Tay, Balasubramanian Murugesapandian, Yunpeng Lu, Rakesh Ganguly, Kinjo Rei and Dragoslav Vidović*

The synthesis, characterization and X-ray analysis of dichloro- and dibromo-borenum cations stabilized by a 4-membered carbene are reported. The ligand's structural changes, atypical for similar systems, were caused by coordination to electron deficient fragments and its CN₂P ring strain.

Introduction

The synthesis and reactivity of group 13 monocations, especially three coordinate borenum cations, have recently gained considerable interest.^{1–11} These boron species were predominantly stabilized by N-heterocyclic carbenes (NHC, **A**, Fig. 1),^{2a–g,4a,7} tertiary amines (**B**)^{2l,3a–d,4b,6b} and various pyridines (**C**),^{2g–h,3f,5,6b} and have been used for borylation,³ hydroboration,⁴ haloborylation,⁵ hydrosilylation,⁶ hydrogenation⁷ and Diels–Alder transformations⁸ of a diverse range of substrates. With respect to NHC-stabilized borenum cations, five-membered NHCs (**A**, $n = 1$, Fig. 1) have been mostly used while an example of a six-membered NHC-stabilized (**A**, $n = 2$) borenum cation was also reported.²ⁱ In this work we wish to communicate the synthesis and characterization of a couple of dihaloborenum cations stabilized by a 4-membered carbene ligand containing a phosphine moiety in its backbone (**D**, Fig. 1).¹²

Results and discussion

Even though free carbene **D** (Fig. 1) has been isolated and fully characterized, we found it extremely difficult to handle.^{12a} Thus, the carbene was prepared and used *in situ* by deprotona-

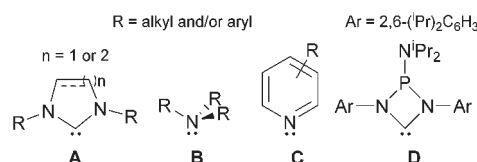
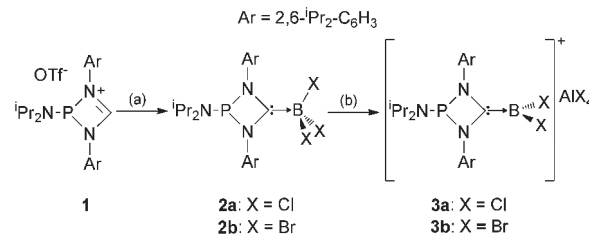


Fig. 1 Most common neutral donor ligands (**A**, **B** and **C**) used for stabilization of borenum cations and the 4-membered carbene (**D**) explored in this work.



Scheme 1 General synthetic procedure. Reaction conditions: (a) 1.1 equiv. of $K[N(SiMe_3)_2]$ in toluene, hexane, 0.57 equiv. BX_3 . (b) 1.0 equiv. of AlX_3 with respect to **2a/2b**, DCM.

tion of iminium salt **1** in toluene (Scheme 1).^{12b} After addition of hexane and filtration, either BCl_3 or BBr_3 was added, resulting in the immediate formation of a white precipitate. The δ_B values for these two individual products were typical for other systems containing neutral NHC–borane adducts (δ_B –0.2 and –17.5 ppm for **2a** and **2b**, respectively, Scheme 1) and other 4-coordinate boron species, eliminating the possibility of spontaneous halide extrusion observed for a borenum cation stabilized by an *ortho*-substituted pyridine.^{2d–g,13} The δ_p values for **2a** (126.5 ppm) and **2b** (128.3 ppm) were upfield shifted with respect to the same signal observed for **1** (135.0 ppm) but in good agreement with a ruthenium complex containing the same ligand.¹²

Furthermore, compound **2a** was crystallographically characterized (Fig. 2) and the values for the B1–C1 (1.633(6) Å) and

SPMS-CBC, Nanyang Technological University, 21 Nanyang Link, 637371, Singapore.
E-mail: dvidovic@ntu.edu.sg; Fax: (+65) 6791 1961

† Electronic supplementary information (ESI) available: Full experimental details, summary of crystallographic data including CIF and DFT. CCDC 986260–986262. For ESI and crystallographic data in CIF or other electronic format see DOI: 10.1039/c4dt01210k

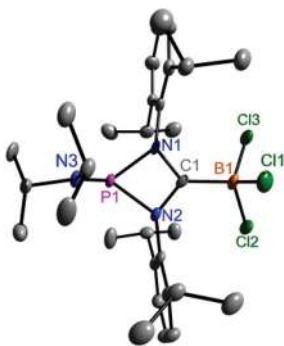


Fig. 2 Molecular structure of **2a**. Thermal ellipsoids have been drawn at the 30% probability level. All hydrogen atoms and disordered solvent molecules have been omitted for clarity.

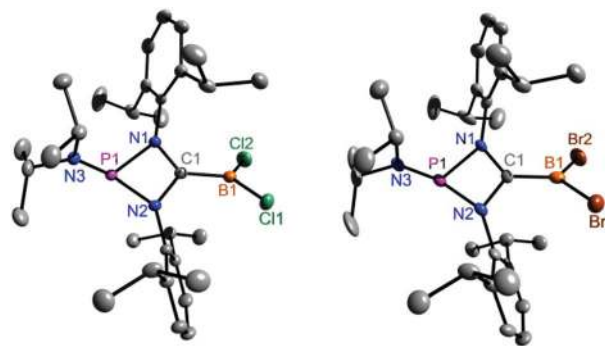


Fig. 3 Molecular structures of **3a** (left) and **3b** (right). Thermal ellipsoids have been drawn at the 30% probability level. All hydrogen atoms and the counterion for both structures have been omitted for clarity.

the average B–Cl (1.847(7) Å) bond distances are typical for analogous compounds.^{2d} The NCN bond angle (101.7(3)°) is slightly larger than the corresponding angle observed for the already mentioned ruthenium complex incorporating this carbene ligand.^{12b} Also, the non-planarity of the cyclic CN₂P fragment was manifested by the values for the sum of the angles around the endocyclic nitrogen atoms of ~352° (Table 1 and Fig. 2), which is consistent with the analogous values observed for other compounds containing this particular fragment.¹²

As expected, introducing 1.0 equiv. of AlCl₃/AlBr₃ into a DCM solution containing **2a/2b** resulted in the formation of the target borenium cations **3a/3b** (Scheme 1) as is evident from the δ_B values of 48.4 and 48.0 ppm, respectively, which are in excellent agreement with analogous borenium cations.^{2d,g} Formation of the corresponding counterions (the δ_{Al} values of 106.3 and 84.0 ppm for AlCl₄⁻ and AlBr₄⁻, respectively) was also detected by ²⁷Al NMR spectroscopy. Additionally, ³¹P NMR spectroscopy provided more evidence for depleted electron density at the newly formed cationic compounds as the δ_P values for **3a** (135.5 ppm) and **3b** (136.1 ppm) were downfield shifted with respect to the precursors (**2a**: δ_P 126.5 ppm; **2b**: δ_P 128.3 ppm). Both cations have also been elucidated by single crystal X-ray diffraction (Fig. 3). The expected B–C1 and the average B–X (X = Cl, Br) bond distance shorten-

ings were observed with regard to **2a** and other known precursors.^{2d,g} The NCN bond angles for **3a** and **3b** are slightly larger than the same angle observed for **2a**. The angles defined by the BX₂ and CN₂ planes are virtually identical for both cations (47.6° and 47.3° for **3a** and **3b**, respectively) suggesting that this particular angle is governed by the steric encumbrance of the carbene substituents. Furthermore, the solid state structures showed no evidence for cation–anion interactions as the shortest B⋯X_(anion) (**3a**: 5.18 Å; **3b**: 5.21 Å) distance for both ionic species was well outside the sum of the van der Waals radii for B and X (vdW_(B–Cl) = 3.73 Å; vdW_(B–Br) = 3.77 Å).¹⁴

However, the most intriguing observation about the solid state analysis for both cations was planarity of one of the endocyclic N atoms and noticeably different values for the P–N bond distances. The sum of the angles around N1 for both borenium cations is exactly 360° while for the other endocyclic N atom (N2 for both compounds) the sum is around 345° (Table 1). In fact, according to X-ray analyses all systems containing this ligand, including the free ligand, exhibited different degrees of pyramidalization at the endocyclic N atoms but none of them, apart from **3a** and **3b**, had one of the N atoms strictly planar.¹² It is noteworthy that solid state analysis of the ruthenium complex containing this ligand revealed that one of the N atoms is almost planar suggesting similar electronic properties between the ruthenium fragment and

Table 1 Selected experimental and theoretical structural parameters for the free ligands, **2a**, **3a** and **3b**

	Bond distances (Å)					Angles (°)			Sum of endocyclic CN ₂ P
	B1–C1	C–N _(average)	B1–X _(average)	P1–N1	P1–N2	NCN	Sum at N1	Sum at N2	
2a	1.633(6)	1.359(6)	1.874(5)	1.794(3)	1.813(3)	101.7(3)	351.6(3)	351.6(3)	357.5(4)
2a ^a	1.645	1.363	1.868	1.807	1.840	101.6	355.3	352.4	357.4
3a	1.586(3)	1.342(3)	1.715(2)	1.787(2)	1.852(2)	103.6(2)	360.0(2)	344.8(2)	357.6(3)
3a ^a	1.594	1.346	1.739	1.826	1.903	104.8	348.3	359.2	357.2
3b ^b	1.57(1)	1.343(8)	1.875(8)	1.785(6)	1.862(6)	103.5(6)	360.0(6)	345.3(6)	357.2(8)
Ligand ^{12a}	N/A	1.380(3)	N/A	1.772(2)	1.773(2)	96.7(2)	355.1(3)	348.2(3)	356.4(4)
Ligand ^a	N/A	1.382	N/A	1.803	1.807	97.3	357.8	353.3	357.5

^a Theoretical values for the optimized structures performed with the Gaussian 09 package using the B3LYP method with 6-31(d,p) basis set. ^b The solid state data might not be as reliable as in the other cases due to the poor crystal quality.

BX_2^+ moieties (see below). Furthermore, the P1–N1 (**3a**: 1.787(2) Å; **3b**: 1.785(6) Å) bond distance is considerably shorter than the P1–N2 (**3a**: 1.852(2) Å; **3b**: 1.862(6) Å) while in the other systems two P–N bond distances are virtually identical.¹² Initially, we postulated that these observations were a result of the π electron delocalization along the CNP fragment for **3a** and **3b** rather than the NCN fragment observed for other similar systems.^{2a–g,4a,7,12} However, after careful examination of solid state data for all compounds containing this particular ligand we concluded that the unequal N-pyramidalization and the discrepancy of the endocyclic P–N bond distances were primarily due to the coordination of a more electron deficient species (BCl_3 vs. BCl_2^+) to the carbene ligand and the inherent CN_2P ring strain.

First of all, it was suggested that strict planarization at both N atoms might not be possible due to the CN_2P ring strain.^{12a} Secondly, an increase in the bond angle at the central carbon, known as the carbene angle ($\angle\text{NCN}$ in this case), for 6 valence electron carbenes decreases the HOMO–LUMO gap and, consequently, increases the σ -donating properties of the ligand.¹⁵ Solid state data analysis revealed that the value for the carbene angle systematically increased from 96.7(2)° for the free carbene to 101.7(3)° for **2a** and even further to 103.6(2)° for **3a** presumably to compensate for a more Lewis acidic moiety being coordinated to the ligand (Table 1). It could then be postulated that one of the N atoms planarized in order to increase its electron donation to the central C atom and minimize the effect(s) of the increased electron depletion. Planarization of the second N atom would have resulted in a completely flat CN_2P fragment which, as suggested, might not be possible due to the ring strain. In fact, it seems that the CN_2P fragment tends to keep a constant degree of the ring strain as the sum of the endocyclic angles ($\sim 357^\circ$, Table 1) remains virtually constant regardless of the ligand's structural changes caused by its coordination chemistry.¹²

Density Functional Theory (DFT; using the Gaussian 09 package, B3LYP method and 6-31(d,p) basis set) studies involving the free ligand, **2a** and **3a**, replicated their structural features including the systematic increase in the carbene angle (Table 1) suggesting a decrease in the HOMO–LUMO gap of the ligand moiety.¹⁶ This was confirmed by the energy-only calculations performed using the ligand's coordinates from the solid state analyses of the free ligand, **2a** and **3a**. These calculations illustrated a methodical (i) increase in the energy of the HOMO (–5.076, –4.411 and –4.336 eV for the ligand's coordinates taken from the free ligand, **2a** and **3a**, respectively), (ii) decrease in the energy of the LUMO (0.017, –0.007 and –0.012 eV) and, hence, (iii) decrease in the HOMO–LUMO gap (5.093, 4.404 and 4.324 eV) of the ligand moiety creating not only a better σ -donor but also a better π -acceptor. In fact, decreasing the energy of the unoccupied orbitals seemed to play a key role in increasing the average value for the P–N bond distance. According to the natural bonding orbital (NBO) analysis the average electron population of the P–N antibonding orbitals increased with the coordination of electron deficient species (Table 2) resulting in longer P–N_{ave} bond distances (Table 1).

Table 2 Electron population of the P–N antibonding orbitals as observed by the NBO analysis

	P1–N1	P1–N2
Ligand	0.13959	0.14741
2a	0.11115	0.19573
3a	0.15595	0.28012

Moreover, unequal electron population of the two P–N antibonding orbitals, resulting in noticeably different values for the P–N bond distances observed for the borocations, was thought to be also attributed to the CN_2P ring strain as in the case of the endocyclic N atom flattening. Therefore, coordination of the carbene ligand to electron deficient species forced the ligand to become more nucleophilic by undergoing certain structural changes. These changes were not uniform with respect to the geometry around the endocyclic N atoms and the values for the P–N bond distances presumably due to the restriction in the CN_2P ring strain.

In summary, we have successfully prepared dichloro- and dibromo-borenium cations stabilized by a four-membered NHC containing a P atom in its endocyclic backbone. Single crystal X-ray diffraction analysis and theoretical studies suggested that the observed non-uniform CN_2P ring-based structural changes of the carbene moiety for the borocations were a result of the coordination of electron deficient moieties BX_2^+ (X = Cl, Br) and the CN_2P ring strain.

Acknowledgements

We would like to thank A*STAR (grant number 1321202066) for financial support.

References

- For recent reviews on boron cations, see: (a) W. E. Piers, S. C. Bourke and K. D. Conroy, *Angew. Chem., Int. Ed.*, 2005, **44**, 5016–5036; (b) S. De Vries, A. Prokofjevs and E. Vedejs, *Chem. Rev.*, 2012, **112**, 4246–4282.
- For recent examples of borenium cations, see: (a) T. Matsumoto and F. P. Gabbaï, *Organometallics*, 2009, **28**, 4252–4253; (b) D. McArthur, C. P. Butts and D. M. Lindsay, *Chem. Commun.*, 2011, **47**, 6650–6652; (c) A. Solovyev, S. J. Geib, E. Lacôte and D. P. Curran, *Organometallics*, 2012, **31**, 54–56; (d) S. Muthaiah, D. C. H. Do, R. Ganguly and D. Vidović, *Organometallics*, 2013, **32**, 6718–6724; (e) Y. Wang, M. Y. Abraham, R. J. Gilliard, D. R. Sexton, P. Wei and G. H. Robinson, *Organometallics*, 2013, **32**, 6639–6642; (f) D. C. H. Do, S. Muthaiah, R. Ganguly and D. Vidović, *Organometallics*, 2014, **33**, 4165–4168; (g) H. B. Mansaray, A. D. L. Rowe, N. Phillips, J. Niemeyer, M. Kelly, D. A. Addy, J. I. Bates and S. Aldridge, *Chem. Commun.*, 2011, **47**, 12295–12297; (h) I. Ghesner, W. E. Piers, M. Parveza and R. McDonald, *Chem. Commun.*,

- 2005, 2480–2482; (i) C. W. Chiu and F. P. Gabbaï, *Organometallics*, 2008, **27**, 1657–1165; (j) E. R. Clark and M. J. Ingleson, *Organometallics*, 2013, **32**, 6712–6717; (k) E. R. Clark, A. Del Grosso and M. J. Ingleson, *Chem. – Eur. J.*, 2013, **19**, 2462–2466; (l) A. Prokofjevs, J. W. Kampf, A. Solovyev, D. P. Curran and E. Vedejs, *J. Am. Chem. Soc.*, 2013, **135**, 15686–15689; (m) M. A. Dureen, A. Lough, T. M. Gilbert and D. W. Stephan, *Chem. Commun.*, 2008, 4303–4305; (n) C. Bonnier, W. E. Piers, M. Parvez and T. S. Sorensen, *Chem. Commun.*, 2008, 4593; (o) D. Vidovic, G. Reeske, M. Findlater and A. H. Cowley, *Dalton Trans.*, 2008, 2293–2297; (p) C. Jones, D. P. Mills, A. Stasch and W. D. Woodul, *Main Group Chem.*, 2010, **9**, 23–30; (q) B. Inés, M. Patil, J. Carreras, R. Goddard, W. Thiel and M. Alcarazo, *Angew. Chem., Int. Ed.*, 2011, **50**, 8400–8403; (r) C. I. Someya, S. Inoue, C. Präsang, E. Irran and M. Driess, *Chem. Commun.*, 2011, **47**, 6599–6601; (s) E. Tsurumaki, S. Hayashi, F. S. Tham, C. A. Reed and A. Osuka, *J. Am. Chem. Soc.*, 2011, **133**, 11956–11959.
- 3 For recent examples of borenium cations in borylation, see: (a) T. S. De Vries, A. Prokofjevs, J. N. Harvey and E. Vedejs, *J. Am. Chem. Soc.*, 2009, **131**, 14679–14687; (b) A. Del Grosso, P. J. Singleton, C. A. Muryn and M. J. Ingleson, *Angew. Chem., Int. Ed.*, 2011, **50**, 2102–2106; (c) S. A. Solomon, A. Del Grosso, E. R. Clark, V. Bagutski, J. J. W. McDouall and M. J. Ingleson, *Organometallics*, 2012, **31**, 1908–1916; (d) V. Bagutski, A. Del Grosso, J. A. Carrillo, I. A. Cade, M. D. Helm, J. R. Lawson, P. J. Singleton, S. A. Solomon, T. Marcelli and M. J. Ingleson, *J. Am. Chem. Soc.*, 2013, **135**, 474–487; (e) A. Del Grosso, R. G. Pritchard, C. A. Muryn and M. J. Ingleson, *Organometallics*, 2010, **29**, 241–249; (f) A. Del Grosso, M. D. Helm, S. A. Solomon, D. Caras-Quintero and M. J. Ingleson, *Chem. Commun.*, 2011, **47**, 12459–12461; (g) M. J. Ingleson, *Synlett*, 2012, 1411–1415; (h) T. Stahl, K. Müther, Y. Ohki, K. Tatsumi and M. Oestreich, *J. Am. Chem. Soc.*, 2013, **135**, 10978–10981.
- 4 For recent examples of borenium cations in hydroboration, see: (a) A. Prokofjevs, A. Boussonnière, L. Li, H. Bonin, E. Lacôte, D. P. Curran and E. Vedejs, *J. Am. Chem. Soc.*, 2012, **134**, 12281–12288; (b) P. Eisenberger, A. M. Bailey and C. M. Crudden, *J. Am. Chem. Soc.*, 2012, **134**, 17384–17387; (c) B. Bentivegna, C. I. Mariani, J. R. Smith, S. Ma, A. L. Rheingold and T. J. Brunker, *Organometallics*, 2014, **33**, 2820–2830.
- 5 For a recent example of borenium cations in haloboration, see: J. R. Lawson, E. R. Clark, I. A. Cade, S. A. Solomon and M. J. Ingleson, *Angew. Chem., Int. Ed.*, 2013, **52**, 7518–7522.
- 6 For recent examples of borenium cations in hydrosilylation: (a) J. Chen, R. A. Lalancette and F. Jaekle, *Chem. Commun.*, 2013, **49**, 4893–4895; (b) S. E. Denmark and Y. Ueki, *Organometallics*, 2013, **32**, 6631–6634.
- 7 For borenium cations in hydrogenation: J. M. Farrell, J. A. Hatnean and D. W. Stephan, *J. Am. Chem. Soc.*, 2012, **134**, 15728–15731.
- 8 For borenium cations in Diels–Alder reactions: Q.-Y. Hu, G. Zhou and E. J. Corey, *J. Am. Chem. Soc.*, 2004, **126**, 13708.
- 9 For examples of cationic aluminium species, see: (a) L. F. Tietze, A. Schuffenhauer and P. R. Schreiner, *J. Am. Chem. Soc.*, 1998, **120**, 7952; (b) Y.-H. Lam, P. H.-Y. Cheong, J. M. Blasco Mata, S. J. Stanway, V. Gouverneur and K. N. Houk, *J. Am. Chem. Soc.*, 2009, **131**, 1947–1957.
- 10 For recent examples of gallium cations, see: (a) S. Tang, J. Monot, A. El-Hellani, B. Michelet, R. Guillot, C. Bour and V. Gandon, *Chem. – Eur. J.*, 2012, **18**, 10239–10243; (b) A. El-Hellani, J. Monot, R. Guillot, C. Bour and V. Gandon, *Inorg. Chem.*, 2013, **52**, 506–514; (c) A. El-Hellani, J. Monot, S. Tang, R. Guillot, C. Bour and V. Gandon, *Inorg. Chem.*, 2013, **52**, 11493–11502; (d) C. Bour, J. Monot, S. Tang, R. Guillot, J. Farjon and V. Gandon, *Organometallics*, 2014, **33**, 594–599.
- 11 For a recent example of an indium cation, see: L.-G. Zhuo, J. J. Zhang and Z.-X. Yu, *J. Org. Chem.*, 2012, **77**, 8527–8540.
- 12 (a) E. Despagnet-Ayoub and R. H. Grubbs, *J. Am. Chem. Soc.*, 2004, **126**, 10198–10199; (b) E. Despagnet-Ayoub and R. H. Grubbs, *Organometallics*, 2005, **24**, 338–340.
- 13 H. Nöth and B. Wrackmeyer, in *Nuclear Magnetic Resonance Spectroscopy of Boron Compounds*, Springer Verlag, Berlin, 1978, ch. 7, pp. 74–101.
- 14 S. Alvarez, *Dalton Trans.*, 2013, **42**, 8617–8636.
- 15 S. Ming-Der and S.-Y. Chu, *Chem. Phys. Lett.*, 1999, **308**, 283–288.
- 16 The HOMO is mainly the σ -lone pair orbital on the central carbon atom while the formally empty p-orbital on the same carbon atom is involved in the formation of the LUMO. For more details see the ESI.†